



Direct and indirect studies of the electrocaloric effect in single crystalline ferrielectric $(\text{NH}_4)_2\text{SO}_4$



V.S. Bondarev^{a,b}, E.A. Mikhaleva^a, M.V. Gorev^{a,b}, I.N. Flerov^{a,b,*}

^a Kirensky Institute of Physics, Federal Research Center KSC SB RAS, 660036 Krasnoyarsk, Russia

^b Institute of Engineering Physics and Radioelectronics, Siberian Federal University, 660074 Krasnoyarsk, Russia

ARTICLE INFO

Article history:

Received 27 May 2021

Received in revised form 12 August 2021

Accepted 25 September 2021

Available online 28 September 2021

Keywords:

Ferrielectric

Electrocaloric effect

Phase transition

Entropy

ABSTRACT

The influence of an electric field on the phase transition parameters and the electrocaloric response in ferrielectric $(\text{NH}_4)_2\text{SO}_4$ was studied using a universal multifunctional adiabatic calorimeter. The very low sensitivity of the phase transition temperature to the electric field, $dT_0/dE \approx 5 \cdot 10^{-3}$ K/(kV/cm), was shown to be the reason for the low maximum value of the intensive electrocaloric effect, ΔT_{AD} , at $E = 11$ kV/cm: direct and indirect measurements gave the values of 0.01 K and 0.05 K, respectively. However, the extensive electrocaloric response revealed by an analysis of the entropy–temperature–electric field phase diagram was relatively large, with a value of $\Delta S_{ECE} \approx -19$ J/kg K, due to the significant contribution of a jump in the excess entropy to the total value, $\delta S_0/\Delta S_0 \sim 0.37$. An additional irreversible increase in temperature under the electric field was associated with the joule effect and indicated a significant electrical conductivity of ammonium sulphate.

© 2021 Elsevier B.V. All rights reserved.

1. Introduction

The increased attention paid by researchers and engineers to the development of cooling devices that are alternatives to the traditional vapour compression technique is associated with at least two environmental problems: the depletion of the ozone layer and global warming [1]. Currently, one of the most popular and promising avenues for research is the design of cooling cycles with solid state refrigerants that undergo phase transitions and demonstrate large caloric effects (CEs). These effects are reversible changes in the entropy/temperature of materials under the action of an external field Y (electric, magnetic, uniaxial/hydrostatic pressure: $\Delta S_{CE} = \int (\partial X / \partial T)_Y dY$; $\Delta T_{AD} = - \int (T/C_p)(\partial X / \partial T)_Y dY$, where X and C_p are the phase transition parameter and the heat capacity, respectively.

A large number of studies have focused on CEs of various physical origins, such as magneto(MCE) -, baro(BCE)/piezo(PCE) - and electro (ECE)-caloric effects [2–8]. ECE, which is associated with the simplest way of implementing the external field, has been actively studied in various ferroelectric materials, including crystals has been

actively investigated in various ferroelectric materials, including crystals, ceramics, films, composites, multilayer structures, and polymer materials [3,9–14]. Ferroelectrics are also sensitive to changes in external pressure, and attention has recently been paid to BCE and PCE in some of these materials, including ammonium sulphate, $(\text{NH}_4)_2\text{SO}_4$ (AS). This belongs to a very rich family of crystals with a structure of the type $\beta\text{-K}_2\text{SO}_4$ (sp. gr. Pnam), and undergoes a phase transition to the ferroelectric phase $\text{Pna}2_1$ at a temperature $T_0 \approx 223$ K [15–18]. One of the specific features of AS is the unusual temperature behavior of spontaneous polarization, P_s , which reaches a certain maximum value at a temperature not much lower than T_0 , and then decreases with further cooling and even changes its sign, which is atypical for traditional ferroelectrics [19]. This feature is explained by the presence of two sublattices in the structure of AS in which polarisation occurs at the same temperature, T_0 , and is characterised by opposite signs and different temperature dependences [20,21]. Experiments have recorded the resulting uncompensated polarisation, which is the algebraic sum of the polarisations of the sublattices. AS is therefore often referred to as a ferrielectric. This is also very likely to be the reason for the unusual behaviour of the permittivity in the paraelectric phase, which shows a slow increase as the temperature decreases towards T_0 [18,22,23].

Although a large number of papers have been devoted to the physical properties and modelling of the mechanism of the unusual dependence $P_s(T)$ in AS [16], researchers have not studied CEs in this

* Correspondence to: Kirensky Institute of Physics, Akademgorodok, 50, bld. 38, Krasnoyarsk 660036, Russia.

E-mail addresses: vbondarev@yandex.ru (V.S. Bondarev), katerina@iph.krasn.ru (E.A. Mikhaleva), gorev@iph.krasn.ru (M.V. Gorev), flerov@iph.krasn.ru (I.N. Flerov).

ferrielectric. This is rather strange, since the high entropy of the phase transition ($\Delta S_0 = 17.7 \text{ J/mol K}$) [18,24,25], considered to be the limiting value of ΔS_{CE} , indicates a significant potential caloric efficiency for AS. The high sensitivity of the phase transition temperature to the external field dT_0/dY is no less important, and is also typical of AS, at least with respect to hydrostatic pressure, as the volumetric baric coefficient is quite large ($dT_0/dp \approx -49 \text{ K/GPa}$) [24–26]. Recent initial studies of BCE in AS have reported the possibility of realising considerable values $\Delta S_{BCE} = -\int(\partial V/\partial T)_p dp = 75 \text{ J/kg K}$ and $\Delta T_{AD} = \int(T/C_p)(\partial V/\partial T)_p dp = -10 \text{ K}$ at a fairly low pressure $p = 0.3 \text{ GPa}$ [24,25]. Moreover, due to the significant anisotropy in the thermal expansion of the crystal lattice, the linear baric coefficient $dT_0/d\sigma_a = -100 \text{ K/GPa}$ associated with uniaxial pressure along the ferroelectric axis a turns out to be greater than the sensitivity of AS to the hydrostatic pressure dT_0/dp [27]. As a result, the corresponding PCE exceeds BCE at the same pressure: $\Delta S_{PCE} = -\int(\partial L/\partial T)_{\sigma} d\sigma = 115 \text{ J/kg K}$ and $\Delta T_{AD} = \int(T/C_p)(\partial L/\partial T)_{\sigma} d\sigma = -16 \text{ K}$.

The sensitivity of T_0 to an electric field has not been thoroughly investigated in AS. It has only been postulated that the shift in the phase transition point under the action of the electric field, dT_0/dE , is insignificant [18], meaning that high-intensity electric fields are necessary for the realisation of large values of the extensive ($\Delta S_{ECE} = \int(\partial P/\partial T)_E dE$) and intensive ($\Delta T_{AD} = -\int(T/C_p)(\partial P/\partial T)_E dE$) ECE. It is likely that this is the main reason for the recent interest in ECE in AS. The extensive effect in a single-crystal plate with a thickness of 50 microns was evaluated indirectly by analysing the $P(T, E)$ dependences (determined from the P - E hysteresis loops) within the Maxwell ratio $(\partial S/\partial E)_T/(\partial P/\partial T)_E$ [28]. These experiments were carried out with high fields of 100–400 kV/cm, which led to rather large values for the extensive ($\Delta S_{ECE} = -30 \text{ J/kg K}$) and intensive ($\Delta T_{AD} = 4.5 \text{ K}$) ECE.

In the present paper, we perform an experimental study of a bulk AS single crystal at a fairly low electric field in comparison with [28], to obtain reliable information about: (i) the intensive ECE, determined both directly and indirectly; (ii) the extensive ECE from an analysis of the S - T - E phase diagram; (iii) the influence of the electric field on the temperature and entropy of the phase transition; and (iv) the contribution of Joule heating to the change in the temperature of AS under an electric field, associated with ECE.

2. Experimental

To obtain large single crystals of AS ($\sim 5 \text{ cm}^3$), we used a method of slow evaporation from an aqueous solution at 40°C . Characterisation by X-ray diffraction using a Bruker D8 ADVANCE powder diffractometer ($\text{Cu-K}\alpha$ radiation) and an Axioskop-40 polarising microscope revealed a single-phase structure, uniformity, and orthorhombic symmetry of the samples at room temperature (sp. gr. Pnam , $Z = 4$). Good agreement was found between the unit cell parameters for crystals under study ($a = 7.7868 \text{ \AA}$, $b = 10.6412 \text{ \AA}$, $c = 5.9951 \text{ \AA}$) and those determined earlier [29].

All experiments were carried out on the same rectangular single crystal parallelepiped, with dimensions $9.25 \times 3.52 \times 0.77 \text{ mm}^3$. To carry out dielectric measurements and to study the influence of the electric field on the thermal properties and caloric effects, silver electrodes were deposited on the faces perpendicular to the ferroelectric axis.

A homemade adiabatic calorimeter was used as the main experimental instrument [30]. Due to the versatility of this setup, we were able to carry out parallel high-precision measurements on the same single-crystal sample of the heat capacity at $E = 0$ and $E \neq 0$, the dielectric constant, and the electrocaloric temperature change. Discrete and continuous heating was used to measure the heat capacity of the sample + “furniture” (electrodes + heater + contact grease) system. In the former case, the calorimetric step was varied from 0.3 to 1.5 K ($dT/d\tau = 0.03 \text{ K/min}$), while in the latter case, the system was

heated at a rate of $dT/d\tau = 0.1 \text{ K/min}$. The results of calorimetric measurements recently performed by the present authors on un-electroded crystalline AS [25,27], obtained from the same crystallisation as in this paper, are used in a later section of this paper as basic data to analyse the effect of the electrodes on the samples.

Studies of the permittivity, ϵ , of single-crystal AS were performed at a frequency of 1 kHz using an E7-20 immittance meter for the heating and cooling modes at a rate of $(0.2-1) \text{ K/min}$.

Direct measurements of the intensive ECE under adiabatic conditions, ΔT_{AD} , were carried out using the method applied earlier in the study of triglycine sulphate (TGS) [31]. Due to the design features of the cryostat of the calorimeter, the values of the electric voltage applied to the sample electrodes were limited. We therefore measured $\Delta T_{AD}(T)$ at an electric field strength of 11 kV/cm, a relatively low value in comparison with the 100–400 kV/cm used in [28]. A platinum resistance thermometer attached to the adiabatic screen closest to the sample allowed us to detect the temperature of the sample with high precision. The temperature difference between the thermometer and the sample was monitored using a doubled copper-constantan thermocouple whose output was supplied to the automatic control circuit. The error in determining the value of ΔT_{AD} did not exceed $\pm 10^{-4} \text{ K}$.

3. Results and discussion

The experimental temperature dependences of the heat capacity of the sample + “furniture” system, measured at $E = 0$ ($C_{E=0}(T)$) and $E = 11 \text{ kV/cm}$ ($C_{E \neq 0}(T)$), are shown in Fig. 1(a). Good agreement between these curves was observed over a wide temperature range.

We were mainly interested in the values and behaviour of the anomalous heat capacities $\Delta C_{E=0}(T)$ and $\Delta C_{E \neq 0}(T)$ associated with the phase transition $\text{Pnam} \leftrightarrow \text{Pna}2_1$, which were determined as follows. The dependences $C_{E=0}(T)$ and $C_{E \neq 0}(T)$ were taken significantly below ($T < 140 \text{ K}$) and above ($T > 230 \text{ K}$) T_0 , and were considered to be part of the regular contribution, C_{REG} , consisting of the heat capacities of the crystal lattice, C_{LAT} , of AS and the “furniture”, C_F , and were approximated by a polynomial function. The subsequent interpolation of C_{REG} to the region of 140–230 K allowed us to determine the values of $\Delta C_E = C_E - C_{REG}$. Fig. 1(b) shows the appearance of a distinct difference in the values of the anomalous molar heat capacities $\Delta C_{E=0}$ and $\Delta C_{E \neq 0}$ in the temperature range close to the phase transition point.

This phenomenon can be considered to be associated with an increase in the temperature of the phase transition under the action of an electric field. A detailed examination of the excess enthalpy at $E = 0$ and $E \neq 0$, defined as $\Delta H = \int \Delta C_E dT$, confirms this hypothesis.

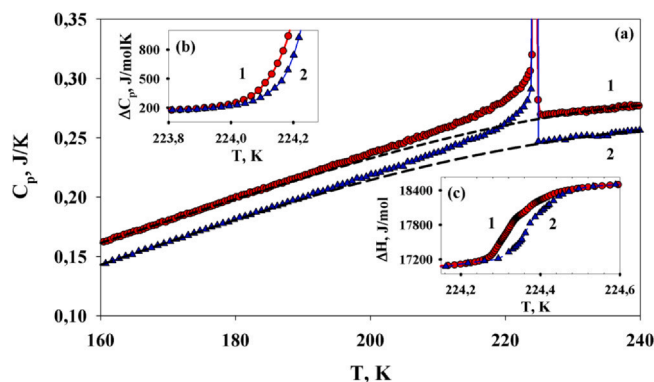


Fig. 1. (a) Temperature dependences of the experimentally measured heat capacities of the sample + “furniture” system at $E = 0$ (curve 1) and $E = 11 \text{ kV/cm}$ (curve 2, shifted down by 0.02 J/K). The dashed lines are nonanomalous contributions. (b) Molar excess heat capacities of AS just below the phase transition temperature. (c) Excess enthalpy near the phase transition point.

Fig. 1(c) shows the behaviour of the function $\Delta H(T)$ in the immediate vicinity of the phase transition point, which is accompanied by the absorption of latent heat corresponding to the enthalpy jump δH_0 , which is smeared under both conditions, $E=0$ and $E \neq 0$, over the same temperature range of ~ 0.15 K. Thus, the electric field does not lead to noticeable additional smearing of the latent heat. At the same time, a small but reliably recorded difference is clearly visible in the phase transition temperatures $T_0^{E=0} = 224.30 \pm 0.01$ K and $T_0^{E \neq 0} = 224.35 \pm 0.01$ K, corresponding to the points of the maximum derivative $(\partial H/\partial T)_E$.

By comparing these results with data from thermographic studies of an AS sample without electrodes [27], in which the absorption of latent heat occurs at an almost constant temperature of $T_0 \pm 0.02$ K, it can be assumed that the smearing of δH_0 observed in our experiments may be due to at least two factors. Firstly, mechanical stresses occur at the contact boundaries of the AS sample and the silver electrodes, due to the difference in their thermal expansion coefficients. The magnitudes and signs of these stresses inevitably vary greatly in the region of T_0 , where the linear dimensions along the b and c axes of the AS sample decrease/increase during cooling/heating due to the anomalous decrease/increase in linear deformation along these axes [27]. Secondly, there is a significant difference between the heating rates of the samples used in this work ($dT/dt \approx 10^{-1}$ K/min) and the ones used in [27] ($dT/dt \approx 6 \times 10^{-3}$ K/min). In our experiments, a rather large value of dT_0/dt leads to a more pronounced temperature gradient inside the AS sample, which is also accompanied by the smearing of T_0 .

However, the magnitudes of the latent heat δH_0 (J/mol) determined at different heating rates and under different electrical conditions are in satisfactory agreement with each other, with values of 1500 ± 120 ($E=0$) and 1480 ± 120 ($E \neq 0$). They also agree with the value obtained for a unelectroded sample of 1450 ± 70 [27]. Thus, the corresponding value of the entropy jump within the limits of error is the same for all cases, i.e. $\delta S_0 = \delta H_0/T_0 = 6.5 \pm 0.5$ J/mol K.

According to the experimental data presented above, the sensitivity of the phase transition to the electric field is very low for AS, with a value of $dT_0/dE = (T_0^{E \neq 0} - T_0^{E=0})/\Delta E \approx 5 \cdot 10^{-3}$ K/(kV/cm). This result is in good agreement with the values estimated using the Clausius-Clapeyron ratio of $dT_0/dE = \delta P_0/\delta S_0 \approx 7 \cdot 10^{-3}$ K/(kV/cm) (where $\delta P_0 = 0.6 \mu\text{C}/\text{cm}^2$ is the jump in polarisation at T_0 [22]), as well as data on $(\partial P/\partial T)_E$, $dT_0/dE \approx 3 \cdot 10^{-3}$ K/(kV/cm) [28]. It is therefore safe to assume that the insignificant value of dT_0/dE is the main reason for the longstanding absence of information on the influence of the electric field on the phase transition in AS.

The value and temperature dependence of the total excess entropy associated with the phase transition was determined by integration of the temperature-dependent part of the anomalous heat capacity and the addition of the jump in entropy at T_0 , i.e. $\Delta S_0 = \int (\Delta C_p/T) dT + \delta S_0$. Fig. 2(a) shows that the value of $\Delta S_0 = 18.0 \pm 0.9$ J/mol K determined in the present paper for $E=0$ and $E \neq 0$ is in good agreement with the results reported in [27].

Summarizing the results above, we can conclude that there is a negligible influence from the electric field on both the changes in entropy, ΔS_0 and δS_0 , in AS, at least up to 11 kV/cm. In combination with the very small value of dT_0/dE , this means that the electric field does not significantly change either the proximity of the phase transition to the tricritical point, or the degree of ordering/disordering of the structural units in the initial and distorted phases. These results reveal that the phase transition in AS is more stable with respect to the electric field than to the hydrostatic pressure. In the latter case [24,25,27], strong decreases under pressure have been observed both in the phase transition temperature and in the jump in entropy, $dT_0/dp = -49$ K/GPa and $d(\delta S_0)/dp \approx 140$ J/(kg K GPa), which leads to a tricritical state ($\delta S_0 = 0$) at a low pressure of ~ 0.35 GPa.

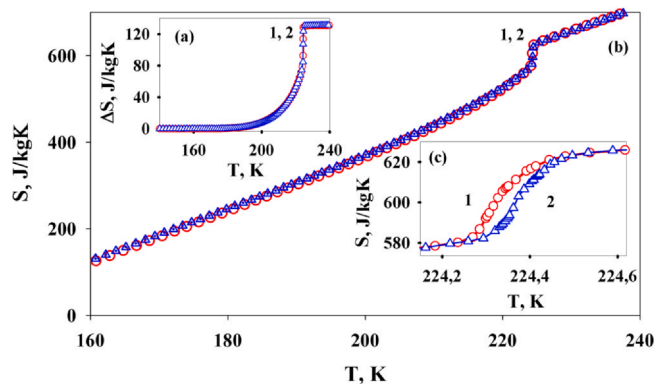


Fig. 2. (a) Total (S) and (b) excess (ΔS_0) entropy over a wide range of temperature at $E=0$ (curve 1) and $E=11$ kV/cm (curve 2); (c) behaviour of S near T_0 .

To determine the electrocaloric properties, we used an approach similar to that applied to the analysis of BCE and PCE in AS [27] and other ferroelectrics [12,32]. The entropy of the crystal lattice, of course, is also stable with respect to the electric field, so to analyse the effect of this field, we used the $S_{\text{LAT}}(T)$ dependence, determined for a sample without electrodes [27], as the background entropy. For both electrical conditions, $E=0$ and $E \neq 0$, the total entropy, $S(T)$, of AS was determined by summing the values of $S_{\text{LAT}}(T)$ [27] and $\Delta S_0(T)$ found in this paper (Fig. 2(b)). The most noticeable difference was observed in the immediate vicinity of the phase transition (Fig. 2(c)).

The value and temperature dependence of the extensive ECE were found as the difference $\Delta S_{\text{ECE}}(T; E) = S(T; E \neq 0) - S(T; E=0)$ at constant temperature. Due to the rather large contribution of the entropy jump to the total value, $\delta S_0/\Delta S_0 \approx 0.37$ (Fig. 2), the function $\Delta S_{\text{ECE}}(T)$ shows a rather narrow but large peak with a maximum of ~ -19 J/kg K (Fig. 3(a)).

The temperature dependence of the intensive ECE was determined by analysing the graph $S(T, E) = S_{\text{LAT}}(T, E=0) + \Delta S_0(T, E)$ at constant entropy, $S(T, E) = S(T) + (\Delta T_{\text{AD}})$, $E=0$ (Fig. 3(b)).

Before taking direct measurements of the intensive ECE in AS, we examined the temperature behaviour of the permittivity and dielectric losses (Fig. 4). When approaching T_0 in the paraelectric phase, the dielectric constant showed a slow increase over a wide temperature range, and then very quickly reached the value of $\epsilon_{\text{max}} \approx 30$. This behaviour of ϵ is similar to that observed earlier [18], where both the shape and the magnitude of the peak of the permittivity depended strongly on repeated thermal cycling, the rate of temperature change, and frequency of the electric field. After several iterations of switching the electric field on and off, the maximum value of the permittivity decreased to $\epsilon_{\text{max}} \approx 35$.

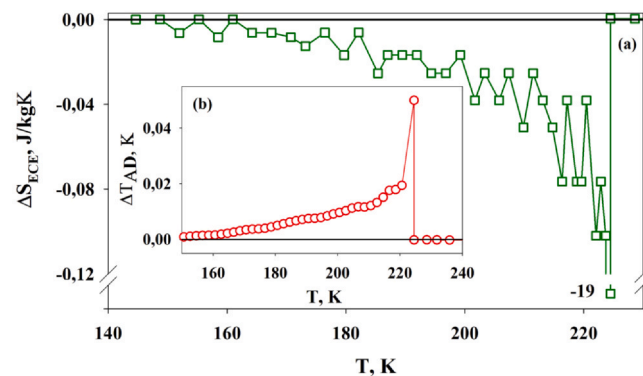


Fig. 3. The behaviour of the (a) extensive ΔS_{ECE} and (b) intensive ΔT_{AD} electrocaloric effects, determined from the dependences $S(T, E)$ shown in Fig. 2(c).

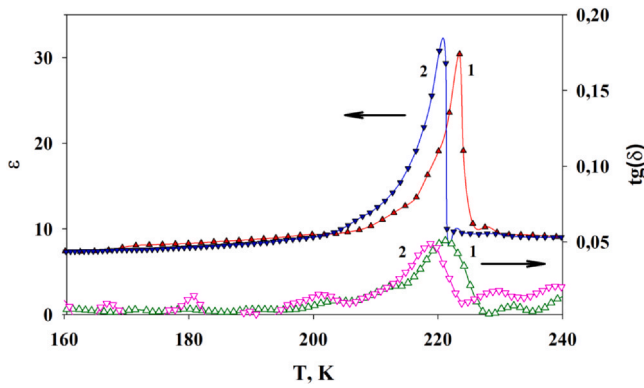


Fig. 4. Temperature dependences of the permittivity and dielectric losses in the heating (curve 1) and cooling (curve 2) modes.

The observed temperature hysteresis, $\delta T_0 \approx 2.8$ K, is comparable to the value found in a previous study of the dependence of the hysteresis on the degree of equilibrium of the measurement conditions, including the heating/cooling rate [25].

In contrast to [28], we also observed an anomalous behaviour of the dielectric losses at the phase transition, where the value of $\text{tg } \delta$ increased to ~ 0.05 at T_0 (Fig. 4), although no increase in $\text{tg } \delta$ was detected on cooling to significantly below T_0 .

Direct measurements of the intensive ECE in AS were performed by switching on and off the electric field, $E = 11$ kV/cm. In the first stage, the sample was heated/cooled to the temperature at which the measurements were to be carried out, and the temperature course (i.e. the rate, $dT/d\tau \approx \pm (1-10) \times 10^{-4}$ K/min, and the linearity in the temperature drift of the sample) was recorded. Fig. 5 shows some results from measuring the time-dependent behaviour of the temperature of the crystal + "furniture" system at different proximities to T_0 .

In all of our experiments, the rate of temperature change at $E = 0$ was low, $dT/d\tau = -(3.3-4.3) \cdot 10^{-4}$ K/min, and constant, corresponding to quasi-adiabatic conditions ($dS \approx 0$). The application of an external

electric field in the immediate vicinity of the phase transition was accompanied by a sharp increase in temperature, $\Delta T_{\text{exp}} = 21 \cdot 10^{-4}$ K (Fig. 5(a)) and $\Delta T_{\text{exp}} = 11 \cdot 10^{-4}$ K (Fig. 5(b)). The temperature drift was not expected to change under $E \neq 0$, but was found to be approximately half as large ($dT/d\tau \approx -(1.0-1.8) \cdot 10^{-4}$ K/min) as at $E = 0$. As a result, after removing the field, the sample temperature did not return to the level that would be expected from an extrapolation of the previous behaviour (Fig. 5(a) and (b)). The difference between the values of $dT/d\tau$ before the field was switched on and after it was switched off did not exceed 10–15%. The same situation was observed for the temperature changes, ΔT_{exp} , in the processes $E \rightarrow 11$ kV/cm and $E \rightarrow 0$, thus demonstrating the high reversibility of the intensive ECE in AS.

In regions further below and above T_0 , no jump in temperature associated with ECE was detected, at least within $\pm 10^{-4}$ K (Fig. 5(c) and (d)). However, the rate of variation in the temperature in the field mode changed significantly, especially for $T > T_0$. When the field was removed, the temperature followed a course parallel to that before the field was applied.

Since the sample under study consists of AS and "furniture", the heat released by the electrocaloric effect is expended in changing the temperature of the system as a whole. Thus, the values of ΔT_{exp} observed in these experiments are lower than the adiabatic temperature changes, ΔT_{AD} , in AS and the relationship between them is given by the following equation:

$$\Delta T_{\text{AD}} = \Delta T_{\text{exp}} \left(1 - \frac{C_F}{C_{\text{AS}}} \right), \quad (1)$$

where C_F (measured in a separate experiment) and C_{AS} are the heat capacities of the "furniture" and the AS crystal, respectively.

Fig. 6(a) shows the temperature dependences of the values of ΔT_{exp} and ΔT_{AD} obtained during the field activation. The maximum value $(T_{\text{AD}})_{\text{max}}^{\text{dir}} \approx 9 \cdot 10^{-3}$ K at $E = 11$ kV/cm is lower than the value $(T_{\text{AD}})_{\text{max}} \approx 50 \cdot 10^{-3}$ K determined from the above analysis of the $S(T)$ function for a different value of E . Nevertheless, these rather small values can be considered close to each other.

In contrast, a rough estimate of the intensive electrocaloric response at 400 kV/cm using the Clausius-Clapeyron equation gives a

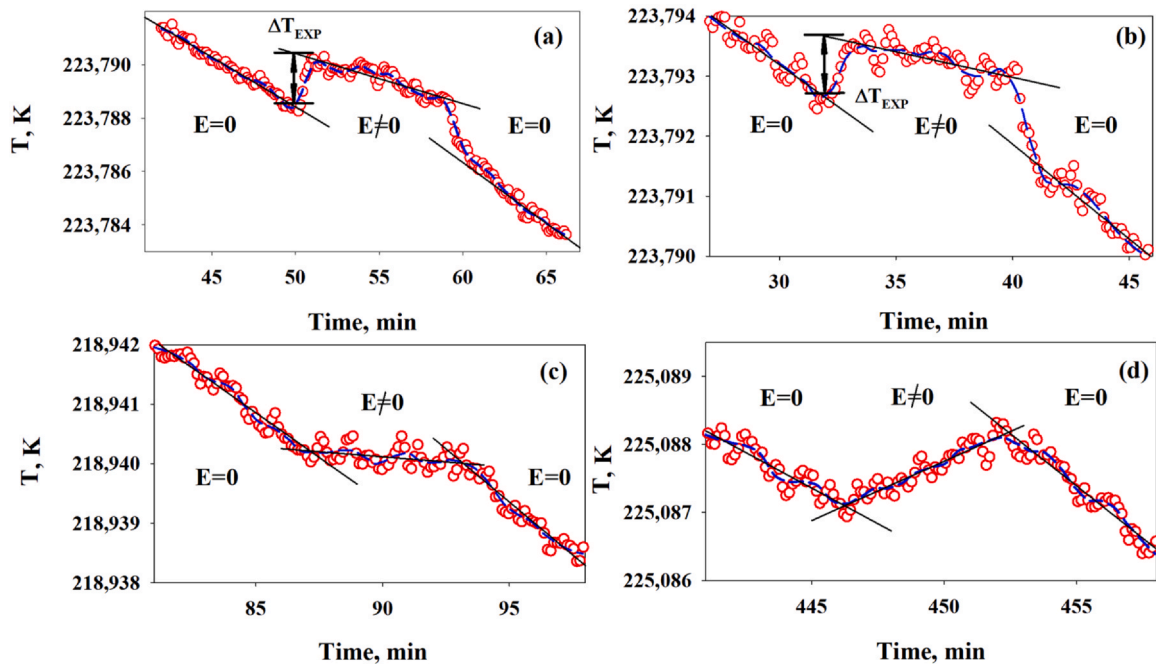


Fig. 5. The time dependence of the temperature of the crystal + "furniture" system in the process of switching on and off the electric field, i.e. ($E = 0$) \rightarrow ($E \neq 0$) \rightarrow ($E = 0$), below and above the phase transition temperature.

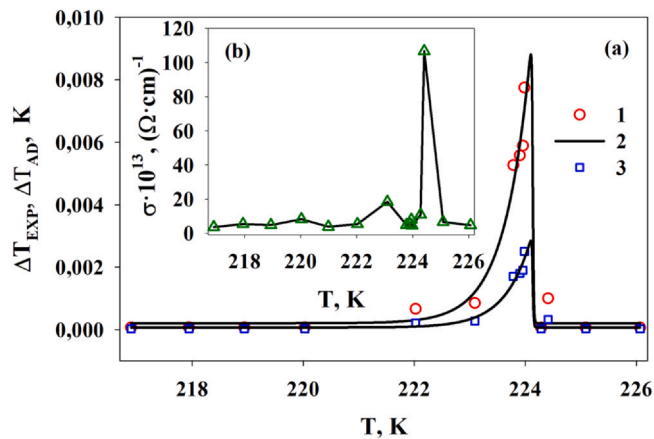


Fig. 6. (a) Temperature dependences of the experimentally measured temperature change, ΔT_{exp} , and the adiabatic temperature change, ΔT_{AD} , recalculated using Eq. (1) for a value of $E = 11$ kV/cm: (1) ΔT_{exp} , (3) ΔT_{AD} ; (2) fit curves; (b) electrical conductivity near the phase transition point.

value of about 4.5 K [28]. Extrapolation of this result to the field used in this work, $E = 11$ kV/cm, gives a value of $\Delta T_{\text{AD}} \approx 120 \times 10^{-3}$ K, which is higher than the magnitudes presented above. In this regard, two points should be noted: firstly, the authors of [28] did not use the jumps in the polarisation and entropy in their calculations of ΔT_{AD} , but instead used “the changes of polarization and entropy across the full transition”; secondly, according to the expression for the enthalpy, $dH = TdS - PdE$, in the case of an isobaric process, the value of the electrocaloric temperature change is determined not by the ratio of the jumps δP_0 and δS_0 , but by the derivative of the function $P(S)$ at $E = \text{const}$, $\Delta T_{\text{AD}} = -\int (\partial P / \partial S)_E dE$.

The results presented here highlight the need for a careful and accurate analysis in the indirect determination of the caloric effects.

At a few degrees below T_0 , the value $(\partial P / \partial T)$ changes sign [22], and the positive sign of the intensive ECE was also expected to change to a negative one. However, we did not observe this phenomenon, and the values of both ΔT_{exp} and ΔT_{AD} decreased very quickly to zero with a decrease in temperature (Fig. 6(a)). Moreover, the value $|(\partial P / \partial T)|$ at $T_0 - 8$ K was significantly lower than at T_0 [22], which can lead to a very small intensive ECE that cannot be detected.

As for the extensive ECE, the value of $\Delta S_{\text{ECE}} \approx -19$ J/kg K (Fig. 3(a)) determined in this work for a low field of 11 kV/cm is worthy of attention. However, due to the very small value of dT_0/dE , an electric field of rather high intensity is required, i.e. $E \approx 65$ kV/cm, to achieve an isothermal entropy change that is at least equal to the entropy jump, $\delta S_0 = -49$ J/kg K. On the other hand, the temperature-dependent part of the phase transition entropy that exists over a very wide range of the ferroelectric phase, $T_0 - 70$ K, will make a significant contribution to the ECE at a much higher field strength, $E \gg 1000$ kV/cm. This assumption is consistent with the results of the electrocaloric analysis of the $P(T, E)$ dependences in [28], where for $E = 400$ kV/cm, ΔS_{ECE} was equal only to ~ -30 J/kg K.

The small value of ΔT_{AD} and the relatively large change in ΔS_{ECE} in AS at a low electric field strength can be associated with the ferroelectric nature of the phase transition. Indeed, the presence of two sublattices in the AS structure with opposite directions of polarisation gives rise to a small value of $\delta P_0 = \delta P_1 + \delta P_2$ and significant changes in entropy, both at the first-order phase transition point $\delta S_0 \sim \delta P_1^2 + \delta P_2^2$ and over a wide temperature range $\Delta S_0 \sim \Delta P_1^2 + \Delta P_2^2$. As a result, the shift of T_0 in the electric field turns out to be insignificant, which leads to small values of ΔT_{AD} . The absence of significant smearing of the jump, δS_0 , even at $E \neq 0$, indicates the possibility of implementing rather large values of ΔS_{ECE} .

We now return to the monotonous heating of the AS sample observed under the action of an electric field (Fig. 5). In this case, the temperature did not return to the initial trajectory after the external field was removed; this suggests a connection with the high electrical conductivity of the AS crystal, which causes the release of Joule heat. The estimates give a rather significant value of $\sigma \approx 5 \cdot 10^{-13} - 10^{-11}$ $(\Omega \cdot \text{cm})^{-1}$ with a maximum near T_0 (Fig. 6(b)), which exceeds the corresponding value of $\sigma = 10^{-16} - 10^{-13}$ $(\Omega \cdot \text{cm})^{-1}$ for the well-known ferroelectric TGS [33]. The irreversible increase in temperature due to the Joule effect poses a serious problem in terms of the implementation of real cooling cycles based on the ECE, as it reduces the resulting efficiency of the solid-state refrigerant [34–37].

The irreversible increase in temperature depends on how long the caloric element is subject to the voltage, while the reversible increase (electrocaloric) does not. Hence, one promising way to solve this problem may be related to the method of implementing ECE in non-equilibrium conditions under a periodically changing electric field [13,31,38].

4. Conclusions

For the first time, thorough experimental studies of the heat capacity $C_p(T)$ of the ferroelectric $(\text{NH}_4)_2\text{SO}_4$ under the conditions $E = 0$ and $E \neq 0$ showed a low sensitivity of the phase transition to the electric field. The shift in the transition temperature at $E = 11$ kV/cm was only ~ 0.05 K. Within the limits of accuracy, the values of the total entropy of the phase transition, $\Delta S_0 = 18.0 \pm 0.9$ J/mol K, and its jump at T_0 , $\delta S_0 = 6.5 \pm 0.5$ J/mol K, turned out to be the same for both types of electrical condition. We can therefore conclude that the influences of the hydrostatic pressure [24,25,27] and the electric field on AS are very different: in the first case, even a low pressure leads to the realisation of the tricritical point, at which $\delta S_0 = 0$.

In the sample with electrodes, the smearing of the entropy jump, δS_0 , was observed over a temperature range of ~ 0.15 K, in contrast to the “unclamped” AS crystal [25,27] in which the release/absorption of latent heat occurred at an almost constant temperature, $T_0 \pm 0.02$ K. This phenomenon may be due to the occurrence of mechanical stresses at the interface between the crystal and the electrodes.

Reasonable agreement between the ECE values derived from two independent methods was established. Indirect determinations of the intensive and extensive effects were carried out by analysing the temperature dependences of the total entropy $S(T)$ at $E = 0$ and $E = 11$ kV/cm, giving values of $\Delta T_{\text{AD}}^{\text{max}} \approx 5 \cdot 10^{-2}$ K and $\Delta S_{\text{ECE}}^{\text{max}} = -19$ J/kg K, respectively. The results of direct ECE measurements in the vicinity of the phase transition under adiabatic conditions, while switching on and off the electric field, were characterised by a high degree of reproducibility. The value of $\Delta T_{\text{AD}}^{\text{max}} \approx 1 \cdot 10^{-2}$ K at $E = 11$ kV/cm was in satisfactory agreement with the value determined indirectly. No change in the sign of ΔT_{AD} was found that would correspond to the observed change in the sign of the derivative $(\partial P / \partial T)_E$ in the temperature range below T_0 [22].

During the $E \neq 0$ process, the sample is irreversibly heated, an effect that is probably due to the high ionic conductivity characteristics of AS [34]. It is hoped that the contribution from the Joule effect to the increase in temperature can be reduced via periodic short-term activation of the electric field [13,31,38].

CRedit authorship contribution statement

V.S. Bondarev: Investigation, Validation, Formal analysis. **E.A. Mikhaleva:** Funding acquisition, Writing – original draft. **M.V. Gorev:** Methodology, Software. **I.N. Flerov:** Conceptualization, Writing – review & editing.

Declaration of Competing Interest

The authors declare that they have no known competing financial interests or personal relationships that could have appeared to influence the work reported in this paper.

Acknowledgements

The reported study was supported by the Russian Science Foundation (project no. 19-72-00023).

References

- [1] A. Greco, C. Aprea, A. Maiorino, C. Masselli, The environmental impact of a caloric heat pump working with solid-state materials based on TEWI analysis, AIP Conf. Proc. 2191 (2019) 020091, <https://doi.org/10.1063/1.5138824>
- [2] L. Mañosa, A. Planes, M. Acet, Advanced materials for solid-state refrigeration, J. Mater. Chem. A 1 (2013) 4925–4936, <https://doi.org/10.1039/C3TA01289A>
- [3] M. Valant, Electrocaloric materials for future solid-state refrigeration technologies, Prog. Mater. Sci. 57 (2012) 980–1009, <https://doi.org/10.1016/j.pmatsci.2012.02.001>
- [4] M. Ožbolt, A. Kitanovski, J. Tušek, A. Poredoš, Electrocaloric refrigeration: thermodynamics, state of the art and future perspectives, Int. J. Refrig. 40 (2014) 174–188, <https://doi.org/10.1016/j.jrefrig.2013.11.007>
- [5] I.N. Flerov, E.A. Mikhaleva, M.V. Gorev, A.V. Kartashev, Caloric and multicaloric effects in oxygen ferroics and multiferroics, Phys. Solid State 57 (2015) 429–441, <https://doi.org/10.1134/S1063783415030075>
- [6] L. Mañosa, A. Planes, Materials with giant mechanocaloric effects: cooling by strength, Adv. Mater. 29 (2017) 1603607, <https://doi.org/10.1002/adma.201603607>
- [7] M. Gorev, E. Bogdanov, I. Flerov, T-p phase diagrams and the barocaloric effect in materials with successive phase transitions, J. Phys. D: Appl. Phys. 50 (38) (2017) 384002, <https://doi.org/10.1088/1361-6463/aa8025>
- [8] N.A. Zarkevich, V.I. Zverev, Viable materials with a giant magnetocaloric effect, Crystals 10 (2020) 815, <https://doi.org/10.3390/cryst10090815>
- [9] X. Moya, E. Stern-Taulats, S. Crossley, D. González-Alonso, S. Kar-Narayan, A. Planes, L.L. Mañosa, N.D. Mathur, Giant electrocaloric strength in single-crystal BaTiO₃, Adv. Mater. 25 (2013) 1360–1365, <https://doi.org/10.1002/adma.201203823>
- [10] F. Lia, J. Lib, Sh Lib, T. Lic, R. Sic, Ch Wang, J. Zhai, Tuning the electrocaloric effect in 0.94Bi_{0.5}Na_{0.5}TiO₃-0.06BaTiO₃ ceramics by relaxor phase blending, Ceram. Int. 46 (2020) 4454–4461, <https://doi.org/10.1016/j.ceramint.2019.10.171>
- [11] A.S. Mischenko, Q. Zhang, J.F. Scott, R.W. Whatmore, N.D. Mathur, Giant electrocaloric effect in thin-film PbZr_{0.95}Ti_{0.05}O₃, Science 311 (2006) 1270–1271, <https://doi.org/10.1126/science.1123811>
- [12] E.A. Mikhaleva, I.N. Flerov, E.V. Bogdanov, V.S. Bondarev, M.V. Gorev, E. Rysiakiewicz-Pasek, Size effect on sensitivity to external pressure and caloric effects in TGS: ceramics and nanocomposites, Mater. Today Commun. 25 (2020) 101463, <https://doi.org/10.1016/j.mtcomm.2020.101463>
- [13] V.S. Bondarev, I.N. Flerov, M.V. Gorev, E.I. Pogoreltsev, M.S. Molokeev, E.A. Mikhaleva, A.V. Shabanov, A.V. Es'kov, Intensive electrocaloric effect in the multilayer capacitor under equilibrium and nonequilibrium thermal conditions, Scr. Mater. 146 (2018) 51–54, <https://doi.org/10.1016/j.scriptamat.2017.06.022>
- [14] B. Neese, B. Chu, S.-G. Lu, Y. Wang, E. Furman, Q.M. Zhang, Large electrocaloric effect in ferroelectric polymers near room temperature, Science 321 (2008) 821–823, <https://doi.org/10.1126/science.1159655>
- [15] R.W.G. Wyckoff, Crystal Structures, 2nd ed., John Wiley & Sons, Inc, New York, London, Sydney, 1964.
- [16] K.S. Aleksandrov, B.V. Beznosikov, Strukturnye Fazovie Perehody v Kristallah (Semeistvo Sulfata Kaliya), Nauka, Novosibirsk, Russia, 1993.
- [17] B.T. Matthias, J.P. Remeika, Ferroelectricity in ammonium sulfate, Phys. Rev. 103 (1956) 262, <https://doi.org/10.1103/PhysRev.103.262>
- [18] S. Hoshino, K. Vedam, Y. Okaya, R. Pepinsky, Dielectric and thermal study of (NH₄)₂SO₄ and (NH₄)₂BeF₄ transitions, Phys. Rev. 112 (1958) 405–412, <https://doi.org/10.1103/PhysRev.112.40>
- [19] F. Jona, G. Shirane, Ferroelectric Crystals, Pergamon Press, Oxford – London – New York – Paris, 1962.
- [20] J. Kobayashi, Y. Enomoto, Y. Sato, A phenomenological theory of dielectric and mechanical properties of improper ferroelectric crystals, Phys. Status Solidi (b) 50 (1972) 335–343, <https://doi.org/10.1002/psb.2220500139>
- [21] V. Dvorak, Y. Ishibashi, Two-sublattice model of ferroelectric phase transitions, J. Phys. Soc. Jpn. 41 (1976) 548–557, <https://doi.org/10.1143/JPSJ.41.548>
- [22] H.G. Unruh, The spontaneous polarization of (NH₄)₂SO₄, Solid State Commun. 8 (1970) 1951–1954, [https://doi.org/10.1016/0038-1098\(70\)90666-6](https://doi.org/10.1016/0038-1098(70)90666-6)
- [23] K. Ohi, J. Osaka, H. Uno, Ferroelectric phase transition in Rb₂SO₄-(NH₄)₂SO₄ and Cs₂SO₄-(NH₄)₂SO₄ mixed crystals, J. Phys. Soc. Jpn. 44 (1978) 529–536, <https://doi.org/10.1143/JPSJ.44.529>
- [24] P. Lloveras, E. Stern-Taulats, M. Barrio, J.-L. Tamarit, S. Crossley, W. Li, V. Pomjakushin, A. Planes, L. Mañosa, N.D. Mathur, X. Moya, Giant barocaloric effects at low pressure in ferroelectric ammonium sulphate, Nat. Commun. 6 (2015) 8801, <https://doi.org/10.1038/ncomms9801>
- [25] E. Mikhaleva, I. Flerov, M. Gorev, V. Bondarev, E. Bogdanov, Features of the behavior of the barocaloric effect near ferroelectric phase transition close to the tricritical point, Crystals 10 (2020) 51, <https://doi.org/10.3390/cryst10010051>
- [26] S. Tsunekawa, Y. Ishibashi, Y. Takagi, Effect of the hydrostatic pressure on the transition temperature in (NH₄)₂SO₄, J. Phys. Soc. Jpn. 33 (1972) 862, <https://doi.org/10.1143/JPSJ.33.862>
- [27] E. Mikhaleva, M. Gorev, V. Bondarev, E. Bogdanov, I. Flerov, Comparative analysis of elastocaloric and barocaloric effects in single-crystal and ceramic ferroelectric (NH₄)₂SO₄, Scr. Mater. 191 (2021) 149–154, <https://doi.org/10.1016/j.scriptamat.2020.09.030>
- [28] S. Crossley, W. Li, X. Moya, N.D. Mathur, Large electrocaloric effects in single-crystal ammonium sulfate, Philos. Trans. A Math. Phys. Eng. Sci. 374 (2016) 20150313, <https://doi.org/10.1098/rsta.2015.0313>
- [29] I.M. Shmyt'ko, N.S. Afonikova, V.I. Torgashev, Anomalous states of the structure of (NH₄)₂SO₄ crystals in the temperature range 4.2–300 K, Phys. Solid State 44 (2002) 2309–2317, <https://doi.org/10.1134/1.1529929>
- [30] A.V. Kartashev, I.N. Flerov, N.V. Volkov, K.A. Sablina, Adiabatic calorimetric study of the intense magnetocaloric effect and the heat capacity of (La_{0.4}Eu_{0.6})_{0.7}Pb_{0.3}MnO₃, Phys. Solid State 50 (2008) 2115–2120, <https://doi.org/10.1134/S1063783408110188>
- [31] V.S. Bondarev, E.A. Mikhaleva, I.N. Flerov, M.V. Gorev, Electrocaloric effect in triglycine sulfate under equilibrium and nonequilibrium thermodynamic conditions, Phys. Solid State 59 (2017) 1118–1126, <https://doi.org/10.1134/S1063783417060051>
- [32] M.V. Gorev, E.A. Mikhaleva, I.N. Flerov, E.V. Bogdanov, Conventional and inverse barocaloric effects in ferroelectric NH₄HSO₄, J. Alloy. Compd. 806 (2019) 1047–1051, <https://doi.org/10.1016/j.jallcom.2019.07.273>
- [33] V.M. Gurevich, Electroprovodnost' segnetoelektrikov, Standards Publishing House: Moscow, Russia, 1969.
- [34] J.F. Scott, Electrocaloric materials, Annu. Rev. Mater. Res. 41 (2011) 229–240, <https://doi.org/10.1146/annurev-matsci-062910-100341>
- [35] M. Quintero, L. Ghivelder, F. Gomez-Marlasca, F. Parisi, Decoupling electrocaloric effect from Joule heating in a solid state cooling device, Appl. Phys. Lett. 99 (2011) 232908, <https://doi.org/10.1063/1.3665949>
- [36] M. Quintero, P. Gaztañaga, I. Irurzun, Intrinsic leakage and adsorption currents associated with the electrocaloric effect in multilayer capacitors, Appl. Phys. Lett. 107 (2015) 151901, <https://doi.org/10.1063/1.4933048>
- [37] Y. Liu, J.F. Scott, B. Dkhil, Direct and indirect measurements on electrocaloric effect: recent developments and perspectives, Appl. Phys. Rev. 3 (2016) 031102, <https://doi.org/10.1063/1.4958327>
- [38] V.S. Bondarev, I.N. Flerov, M.V. Gorev, E.I. Pogoreltsev, M.S. Molokeev, E.A. Mikhaleva, A.V. Shabanov, A.V. Es'kov, Influence of thermal conditions on the electrocaloric effect in a multilayer capacitor based on doped BaTiO₃, J. Adv. Dielect. 07 (2017) 1750041, <https://doi.org/10.1142/S2010135X1750041>